Temperature dependence of current-voltage characteristics of Ni–AlGaN/GaN Schottky diodes

Wantae Lim,[1] Jae-Hyun Jeong,[1] Jae-Hoon Lee,[1] Seung-Bae Hur,[1] Jong-Kyu Ryu,[1] Ki-Se Kim,[1] Tae-Hyung Kim,[2] Sang Yeob Song,[2] Jong-In Yang,[2] and S. J. Pearton[3,a)]
[1]*GaN Power Research Group, Samsung LED, Suwon 443-743, South Korea*
[2]*R&D 1 Team, Samsung LED, Suwon 443-743, South Korea*
[3]*Department of Materials Science and Engineering, University of Florida, Gainesville, Florida 32611, USA*

(Received 13 September 2010; accepted 19 November 2010; published online 13 December 2010)

Ni–AlGaN/GaN Schottky barrier diodes (SBDs) with lateral geometry were fabricated on sapphire substrates. At 300 K, devices with 500-μm-diameter Schottky contacts exhibited breakdown voltage (V_B) of 765 V, forward current (I_F) of 0.065 A at 1.5 V, and specific on-resistance (R_{on}) of 81.3 mΩ cm^2, producing a figure-of-merit (V_B^2/R_{on}) of ~7.2 MW cm^{-2}. Measured in multifinger patterns, the same parameters were 420 V, 3.2 A, 4.6 mΩ cm^2, and 38.4 MW cm^{-2}, respectively, at 300 K. With the increase in measurement temperature from 300 to 450 K, SBDs with dimensions of 3000×3000 μm^2 showed larger effective barrier heights (0.8 eV at 300 K and 1.27 eV at 475 K) and a slightly negative temperature coefficient (−0.48 V K^{-1}) for reverse breakdown voltage, while there was a little change in reverse leakage current. These results show the strong influence of barrier height inhomogeneity on the temperature dependence of apparent barrier heights obtained through current-voltage measurements. © *2010 American Institute of Physics*.
[doi:10.1063/1.3525931]

There has been extensive interest in wide bandgap semiconductors for high power electronic applications.[1–11] So far, the most commonly used material for power electronics has been silicon carbide (SiC). However, the as-yet nonoptimized thermal oxides on SiC power metal oxide semiconductor field effect transistors (FETs) limit the temperature range of application, as the gate contact degrades and become electrically leaky at high temperatures.[12] Additionally, the low electron mobility (~400 cm^2 V^{-1} s^{-1}) results in low power-added efficiency in the frequency range 1–5 GHz. GaN is superior choice due to its larger bandgap and higher electron mobility. A key aspect of the ability of GaN to be useful at high powers is the temperature dependence of barrier height and current-voltage characteristics in Schottky diodes.

Recently, several research groups have reported on AlGaN/GaN Schottky barrier diodes (SBDs) or heterostructure FETs.[13–16] There are still numerous shortcomings in these devices, including higher reverse leakage currents than expected from thermionic emission models, high forward voltage, negative temperature coefficient for reverse breakdown voltage, nonuniformities, and low thermal conductivity of the sapphire substrates.[17,18] In this letter, we report on the temperature dependence of current-voltage characteristics and apparent barrier height for Ni–AlGaN/GaN-based SBDs with lateral geometry. SBDs with size of 3000×3000 μm^2 exhibited a slightly negative temperature coefficient with a little change in reverse leakage current.

The AlGaN/GaN heterostructures were grown on 2 in. sapphire substrates using metal organic chemical vapor deposition (CVD). trimethylgallium (TMGa), trimethylaluminium (TMAl), and ammonia (NH_3) were used as precursors for GaN and AlGaN growth. A 30-nm-thick GaN was grown at 550 °C as a nucleation layer, followed by $Al_{0.3}Ga_{0.7}N$ (35 nm)/GaN (2.8 μm) layers at 1100 °C. Sheet carrier density of 8×10^{12} cm^{-2} and electron mobility of ~1200 cm^2 V^{-1} s^{-1} were obtained by Hall measurements. The buffer carrier concentration was below 10^{15} cm^{-3}. Prior to fabrication, the samples were dipped in H_2SO_4:H_2O_2 (1:1) solution for 10 min to remove organic contamination. Ohmic contact metals of Ti/Al/Ni/Au (30/120/40/80 nm) were deposited by e-beam evaporation and annealed at 850 °C for 30 s in N_2 ambient. Next, a SiO_x passivation layer (600 nm) was selectively formed on the AlGaN layer using plasma enhanced CVD. Schottky contact metals of e-beam evaporated, unannealed Ni/Al/Au (80/700/160 nm) were defined using photolithography and lift-off processes. The Au acts to prevent oxidation of the other metals and provides a low sheet resistance, the Al is used to provide the best adherence to the Au, and the Ni is used as the gate metal. The Schottky metals partially deposited on the SiO_x film also act as metal field plates with 5-μm-long overlapping in order to improve breakdown voltage. The metal thicknesses have been optimized to provide the best step coverage over the dielectric. Finally, Ti/Al (150/2000 nm) metal stacks were deposited for pad metals. A schematic cross-sectional view of the competed SBD device is shown in Fig. 1.

For theoretical analysis, two dimensional device simulations were performed using SILVACO by ATLAS™, 4701 Patrick Henry Drive, Santa Clara, CA 95054. All the parameters used in the simulation, such as dimensions, metal work function, and specific contact resistance, were the same as those obtained experimentally. Current-voltage (I-V) characteristics were recorded using an Agilent 4155 parameter analyzer and an STI curve tracer 5000E. The Agilent 4155 was used to determine Schottky barrier height and contact resistance while STI curve tracer 5000E was used for high power measurement.

a)Electronic mail: spear@mse.ufl.edu.

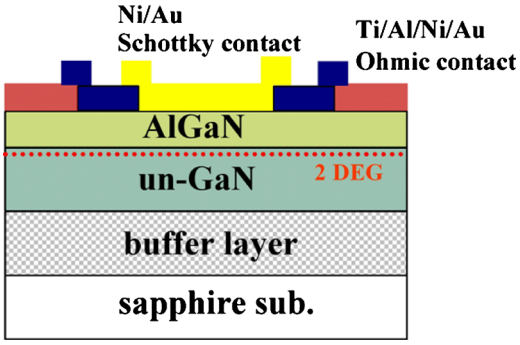

FIG. 1. (Color online) Schematic cross-section of AlGaN/GaN-based SBD device with 500-μm-diameter Schottky contact.

Figure 2 shows the typical forward and reverse *I-V* characteristics at 300 K for the diodes. The diameter of the circular Schottky contact was 500 μm and the distance (L_{ac}) between Ohmic and Schottky contacts was 30 μm. As shown in Fig. 2 (top), the reverse V_B was 765 V, with I_F of 65 mA at 1.5 V. The R_{on} was 81.3 mΩ cm^2, leading to a figure-of-merit (V_B^2/R_{on}) of ~7.2 MW cm^{-2}. The reverse leakage current at V_B was ~200 μA at the breakdown voltage. The corresponding values for multifinger patterned SBDs were 420 V, 3.2 A, 4.6 mΩ cm^2, and 38.35 MW cm^{-2}, respectively (Fig. 2, bottom). The R_{on} of multifinger patterns was reduced by more than one order of magnitude, compared to that measured circular type SBDs. This indicates that the multifinger structures can reduce the contact resistance on AlGaN layer due to good current spreading, resulting in low turn-on voltage.

Figure 3 shows the simulated and experimental *I-V* results at 300 K obtained from multifinger structures with L_{ac} of 30 μm. Table I summarizes the key parameters used in this simulation. The total anode width and device size were 120 mm and 9 mm^2, respectively. The experimental forward

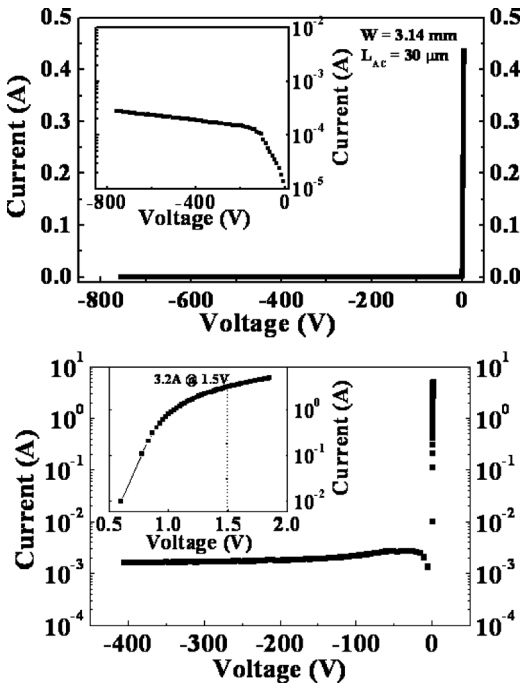

FIG. 2. Typical forward and reverse *I-V* characteristics for AlGaN/GaN-based SBDs with 500-μm-diameter Schottky contacts (top) and multifinger patterned contacts (bottom).

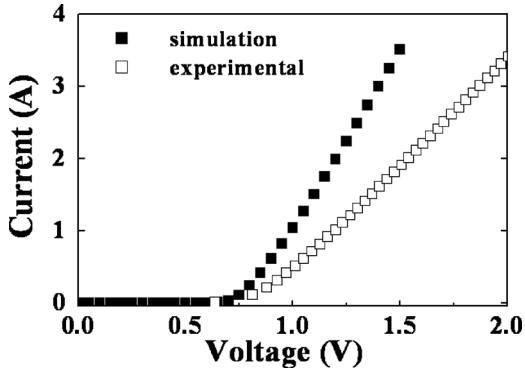

FIG. 3. Simulated and experimental *I-V* results obtained from multifinger SBD structures with the size of 3000×3000 μm^2.

characteristics at 300 K were found to be slightly inferior but very close to the simulation, even though no interface state and defect densities for the AlGaN/GaN structure were assumed in the simulation. The R_{on} calculated from the simulation and experimental results were 4.9 and 7.8 mΩ cm^2, respectively.

Temperature dependent forward *I-V* characteristics for multifinger SBDs with the size of 3000×3000 μm^2 are shown in Fig. 4 (top). As measurement temperature increased from 300 to 475 K, the forward current was increased at low voltage operation (<1.5 V). However, the current was decreased in the range over 1.5 V, due to the reduced carrier mobility. Anwar *et al.*[19] and Oxley *et al.*[20] reported that saturation velocity in AlGaN or AlGaN/GaN is dependent on ambient temperature, which means that electron saturation velocity and electron mobility are reduced at high temperature due to scattering effects, leading to lower on-current.

The *I-V* characteristics based on the thermionic emission theory are given by

$$I = I_s \exp\left(\frac{qV}{nKT}\right)\left[1 - \exp\left(\frac{-qV}{kT}\right)\right], \quad (1)$$

where

$$I_s = AA^*T^2 \exp\left(\frac{-q\phi_b}{KT}\right), \quad (2)$$

and I_s is the saturation current, q is the electric charge, T is the relative temperature, k is the Boltzmann constant, ϕ_b is the Schottky barrier height, A is the contact area, and A^* is the effective Richardson constant. The theoretical value of A^* is calculated from $A^*=4\pi qk^2m^*/h^3$. By using GaN ($0.2m_e$) and AlN ($0.48m_e$) effective masses, the value of A^* was found to be 34.06 A cm^{-2} K^{-2} for $Al_{0.3}Ga_{0.7}N$. Figure 4 (bottom) shows Schottky barrier heights for AlGaN/GaN diodes at different measurement temperatures. The barrier heights were 0.81 eV at room temperature (300 K) and 1.27 eV at 475 K. The corresponding ideality factors were 2.3 at room temperature and 1.4 at 475 K, with a monotonic decrease with temperature. The series resistance showed only small changes in this temperature range. A strong increase in the barrier height with measurement temperature cannot be explained theoretically. This phenomenon is commonly observed in real Schottky diodes and attributed to the Schottky barrier height inhomogeneity.[21,22] The current of Schottky barrier diodes will preferentially flow through the lower bar-

TABLE I. Key parameters used in simulation.

	Metal work function (eV)	Field plate overlap (μm)	Contact resistance (Ω cm^{-2})	Sheet carrier density ($\times 10^{12}$ cm^{-2})	Carrier mobility (cm^2 V^{-1} s^{-1})	
Simulation	5.1	5	5×10^{-5}	8	1200	No traps
Experimental	5.1	5	5×10^{-5}	7.8	~1200	Traps

riers at low temperature. However, as the temperature increases, electrons gain sufficient thermal energy to surmount the higher barriers. Thus, the barrier heights obtained from *T-I-V* characteristics are in good agreement with the Schottky barrier height inhomogeneity model.

Figure 5 shows the reverse leakage current of the multifinger pattered SBDs at different measurement temperatures (300–450 K). The temperature dependence of reverse breakdown was very small, though the temperature coefficient

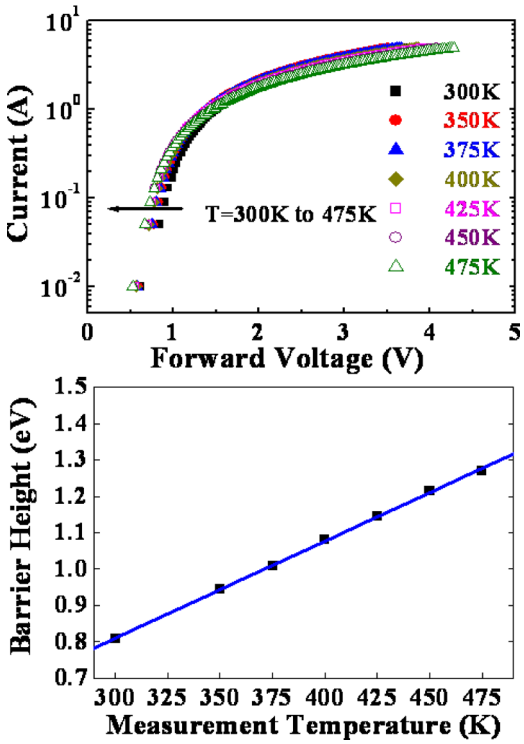

FIG. 4. (Color online) Temperature dependent forward characteristics (top) and Schottky barrier heights (bottom) from multifinger SBDs with the size of 3000×3000 μm^2.

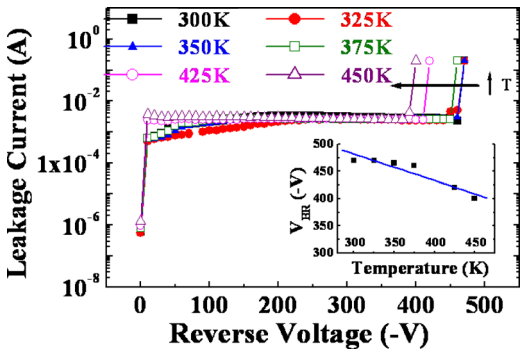

FIG. 5. (Color online) Reverse leakage current of multifinger patterned SBDs at different measurement temperatures.

(-0.48 V K^{-1}) was slightly negative as shown in the inset of Fig. 5. In 4H-SiC or bulk GaN rectifier development, the diodes also showed a negative temperature coefficient and the switch to the positive coefficient was only seen as the defect density in the material was improved.[23] The negative temperature coefficient of the AlGaN/GaN SBDs suggests that the dominant breakdown mechanism for these rectifiers is defect-assisted breakdown.

In conclusion, the temperature dependent measurement showed a slightly negative temperature coefficient of breakdown voltage and a little change in reverse leakage current, which is indicative of a small influence of crystal defects. However, the barrier height data can only be explained by invoking inhomogeneous Schottky contacts.

[1]A. P. Zhang, G. Dang, F. Ren, J. Han, A. Y. Polyakov, N. B. Smirnov, A. V. Govorkov, J. M. Redwing, H. Cho, and S. J. Pearton, Appl. Phys. Lett. **76**, 3816 (2000).
[2]N. Dyakonova, A. Dickens, M. S. Shur, R. Gaska, and J. W. Yang, Appl. Phys. Lett. **72**, 2562 (1998).
[3]J. S. Moon, M. Micovic, A. Kudoghlian, P. Janke, P. Hashimoto, W. S. Wong, L. McCray, and C. Nguyen, IEEE Electron Device Lett. **23**, 637 (2002).
[4]D. Mistele, Mater. Sci. Eng., B **93**, 107 (2002).
[5]M. Ravinandan, P. K. Rao, and V. R. Reddy, Semicond. Sci. Technol. **24**, 035004 (2009).
[6]S. J. Pearton, J. C. Zolper, and R. J. Shul, J. Appl. Phys. **86**, 1 (1999).
[7]U. K. Mishra, P. Parikh, and Y. F. Wu, Proc. IEEE **90**, 1022 (2002).
[8]L. S. McCarthy, P. Kozodoy, M. J. Rodwell, S. P. DenBaars, and U. K. Mishra, IEEE Electron Device Lett. **20**, 277 (1999).
[9]X. A. Cao, A. A. Syed, and H. Piao, J. Appl. Phys. **105**, 063707 (2009).
[10]S. C. Lee, M. W. Ha, J. C. Her, S. S. Kim, J. Y. Lim, K. W. Seo, and M. K. Han, Proceedings of the ISPSD, 2005.
[11]L. Lewis, B. Corbett, D. O. Mahony, and P. P. Maaskant, Appl. Phys. Lett. **91**, 162103 (2007).
[12]K. P. Lee, A. Dabiran, P. P. Chow, S. J. Pearton, and F. Ren, Solid-State Electron. **47**, 969 (2003).
[13]S. Yoshida, J. Li, H. Takehara, H. Kambayashi, and N. Ikeda, Proceedings of the ISPSD, 2006.
[14]D. J. Ewing, M. A. Derenge, P. B. Shah, U. Lee, T. S. Zheleva, and K. A. Jones, J. Vac. Sci. Technol. B **26**, 1368 (2008).
[15]Y. S. Lin, Y. W. Lain, and S. S. H. Hsu, IEEE Electron Device Lett. **31**, 102 (2010).
[16]E. J. Miller, X. Z. Dang, and E. T. Yu, J. Appl. Phys. **88**, 5951 (2000).
[17]A. P. Zhang, J. W. Johnson, B. Luo, F. Ren, S. J. Pearton, S. S. Park, Y. J. Park, and J. I. Chyi, Appl. Phys. Lett. **79**, 1555 (2001).
[18]J. W. P. Hsu, M. J. Manfra, D. V. Lang, S. Richter, S. N. G. Chu, A. M. Sergent, R. N. Kleiman, L. N. Pfeiffer, and R. J. Molnar, Appl. Phys. Lett. **78**, 1685 (2001).
[19]A. F. M. Anwar, S. Wu, and R. T. Webster, IEEE Trans. Electron Devices **48**, 567 (2001).
[20]C. H. Oxley, M. J. Uren, A. Coates, and D. G. Hayes, IEEE Trans. Electron Devices **53**, 565 (2006).
[21]Y. Zhou, D. Wang, C. Ahyi, C. C. Tin, J. Williams, M. Park, N. M. Williams, A. Hanser, and E. A. Preble, J. Appl. Phys. **101**, 024506 (2007).
[22]S.-H. Phark, H. Kim, K. M. Song, P. G. Kang, H. S. Shin, and D.-W. Kim, J. Phys. D: Appl. Phys. **43**, 165102 (2010).
[23]L. F. Voss, B. P. Gila, S. J. Pearton, H. T. Wang, and R. Ren, J. Vac. Sci. Technol. B **23**, 2373 (2005).